

Physicochemical Properties and Time Stability of Plasma Activated Water by a Liquid-Cathode Glow-Type Discharge in Air: The Effect of Air Confinement

Brenda Santamaría¹, Matías G. Ferreyra, Juan C. Chamorro¹, Ezequiel Cejas¹,
Brenda L. Fina, and Leandro Prevosto¹

Abstract—Nonthermal discharges in atmospheric pressure air in contact with water produce large amounts of reactive species in the gas phase that can enter into the water by diffusion, thus inducing the formation of secondary reactive species in the liquid phase, including those long-lived species such as NO_2^- , NO_3^- , and H_2O_2 . Depending on the controllable parameters of the discharge, the plasma activated water (PAW) may acquire different physicochemical properties, resulting in various applications. Physicochemical measurements of PAW obtained by means of a water-cathode glow-type discharge in atmospheric pressure air operating in open and closed reactor conditions are reported. The discharge was operated in a millisecond pulsed-dc regime at an rms current value of 100 mA and a power of 100 W. A large volume of 1 L of distilled water was treated for 30 min. In both cases, low pH values of ~ 2.5 and very high levels of NO_3^- (up to 250 mg/L) in PAW were obtained; however, in the closed system, no H_2O_2 was found and high concentrations of nitrite (120 mg/L) were measured, while in the open system, large levels of H_2O_2 were observed (45 mg/L) and no NO_2^- was found. Likewise, the electrical conductivity value for the closed reactor ($\approx 2000 \mu\text{S}/\text{cm}$) was significantly higher than for the open reactor ($\approx 1000 \mu\text{S}/\text{cm}$). The reasons for these different behaviors in terms of PAW chemistry are discussed. Also, the time stability of PAW was measured.

Index Terms—Nonthermal discharges, plasma activated water (PAW), reactive species in water.

Manuscript received 30 October 2022; revised 22 February 2023 and 28 March 2023; accepted 16 May 2023. This work was supported in part by the Universidad Tecnológica Nacional under Grant PID 8460, in part by the Consejo Nacional de Investigaciones Científicas y Técnicas (CONICET) under Grant PIP 11220200100459CO, and in part by the Agencia Santaferina de Ciencia Tecnología e Innovación under Grant DTT 2021-028. The work of Brenda Santamaría and Matías G. Ferreyra was supported by CONICET through the Doctoral Fellowship. The work of Juan C. Chamorro and Ezequiel Cejas was supported by CONICET through the Post-Doctoral Fellowship. The review of this article was arranged by Senior Editor S. J. Gitomer. (Corresponding author: Brenda Santamaría.)

Brenda Santamaría, Matías G. Ferreyra, Juan C. Chamorro, and Ezequiel Cejas are with the Grupo de Descargas Eléctricas, Departamento Ingeniería Electromecánica, Facultad Regional Venado Tuerto, Universidad Tecnológica Nacional, Venado Tuerto 2600, Argentina (e-mail: brendasantamaria1989@gmail.com).

Brenda L. Fina and Leandro Prevosto are with the Grupo de Descargas Eléctricas, Departamento Ingeniería Electromecánica, Consejo Nacional de Investigaciones Científicas y Técnicas (CONICET), Facultad Regional Venado Tuerto, Universidad Tecnológica Nacional, Venado Tuerto 2600, Argentina.

Color versions of one or more figures in this article are available at <https://doi.org/10.1109/TPS.2023.3281080>.

Digital Object Identifier 10.1109/TPS.2023.3281080

I. INTRODUCTION

PLASMA is a partially or fully ionized gas consisting of a mixture of electrons, ions, and neutral particles, where the amount of positive and negative charges must balance. The most common mode of plasma generation at laboratory scale is by means of the use of electrical discharges in a gas [1], and they are traditionally divided into two broad categories: 1) thermal discharges—the energies of the heavy particles are of the order of the electron energy ($\sim 1 \text{ eV} = 11600 \text{ K}$) [2]—and 2) nonthermal discharges—the electron energy is much higher ($\sim 1\text{--}3 \text{ eV}$) than the energy of heavy particles ($\sim 300\text{--}1000 \text{ K}$) [3].

In recent years, interest in nonthermal discharges in (and in contact with) liquids has been increasing due to their multiple technological applications, covering areas such as nanomaterial deposition, medicine, environmental care, and agriculture, among others [4], [5], [6]. With respect to environmental care, given its ability to decompose organic and inorganic compounds in water, the use of nonthermal plasmas has focused on the degradation of dyes used in various industrial sectors, which are often resistant to traditional treatment processes [7], [8].

Within plasmas in agriculture, the utilization of nonthermal discharges through liquids that have previously been exposed to plasma [such as plasma “activated” water (PAW)] [4] has been focused on seed germination and plant fertilization, pathogen inhibition, and agrochemical degradation, among others [9]. This type of treatment, commonly called “indirect,” has certain advantages over “direct” treatment (where substrates, such as seeds and food, are directly exposed to the discharge), such as the possibility of decoupling the PAW generation site from the application site, as well as the possibility of easily applying it on substrates with complex shapes.

A variety of nonthermal discharges have been used for PAW generation, such as gliding arc, dielectric barrier discharge (DBD), plasma jet, corona discharge, and glow discharge. The composition of the PAW depends on various operating parameters of the discharge, such as type of discharge, type of gas where the discharge is set, and plasma exposure

67 time, whether the discharge is set above or below the water
 68 surface, among others [9]. In air or similar mixtures, the
 69 main species found in water are reactive oxygen and nitrogen
 70 species (RONS), including hydroxyl radical, ozone, superoxide
 71 radical, peroxyxynitrite, nitrate, nitrite, and hydrogen peroxide.
 72 The latter three species—nitrate (NO_3^-), nitrite (NO_2^-), and
 73 hydrogen peroxide (H_2O_2)—have the longest half-lives in
 74 the liquid volume [9], although degradation time scales vary
 75 strongly depending on the pH [10].

76 A widely used nonthermal discharge in contact with liquids
 77 is the glow-type discharge. In air (or other molecular gases)
 78 at atmospheric pressure, the discharge becomes strongly inho-
 79 mogeneous due to the plasma constriction, but the degree of
 80 thermal nonequilibrium is still maintained at high level [9],
 81 resulting in large amounts of RONS [3]. The RONS formed in
 82 the gas phase enters the liquid by diffusion, thus leading to the
 83 formation of reactive species in the volume of the liquid such
 84 as NO_3^- , NO_2^- , H_2O_2 , and hydroxyl radical (OH^\cdot). The cathode
 85 voltage drops reported for water-cathode glow discharges are
 86 higher than their corresponding values for metal electrodes;
 87 this is because the secondary electron emission coefficient of
 88 water is 2–3 orders of magnitude lower than that of a metal
 89 cathode [11].

90 Despite the great interest and importance for practical
 91 purposes, at present, there have not been too many works
 92 characterizing the synthesis of large volumes of PAW (of the
 93 order of 1 L) by means of high-power discharges in air (and
 94 other gases) [12], [13], [14]. This work is an effort to address
 95 this issue.

96 Physicochemical experimental data of distilled water
 97 exposed to a nonthermal high-power glow-type discharge in
 98 atmospheric pressure air with the water being the cathode are
 99 reported. The volume of water treated was 1 L, while the
 100 maximum plasma exposure time reached 30 min. Two variants
 101 (treatments) were employed for the same experimental setup:
 102 1) with the gaseous chamber where the glow discharge is set
 103 confined (closed reactor) and 2) with the open chamber (open
 104 reactor). In particular, pH values, electrical conductivity, and
 105 aqueous phase concentrations of NO_3^- , NO_2^- , and H_2O_2 are
 106 reported. Also, the time stability of PAW up to three months
 107 was measured.

108 II. PLASMA REACTOR

109 A schematic of the plasma reactor is presented in Fig. 1.
 110 A photograph of the discharge with liquid cathode is also
 111 shown. A pin-to-water electrode configuration was used, with
 112 a gaseous gap ≈ 10 mm. A needle shape (a tip radius of about
 113 $200 \mu\text{m}$) of thoriaated tungsten metal electrode (anode) was
 114 placed above the water to be treated, which was contained in
 115 a grounded reservoir of 1-L capacity made of AISI 304.

116 In order to increase the gas–liquid exchange surface and
 117 improve the mixing of the species that enter in the liquid
 118 volume, a vortex was generated with a magnetic stirrer. This
 119 also allowed the evaporation processes in the cathode spot
 120 to be negligible. In this sense, to avoid heating the PAW,
 121 the temperature of the water during the activation process

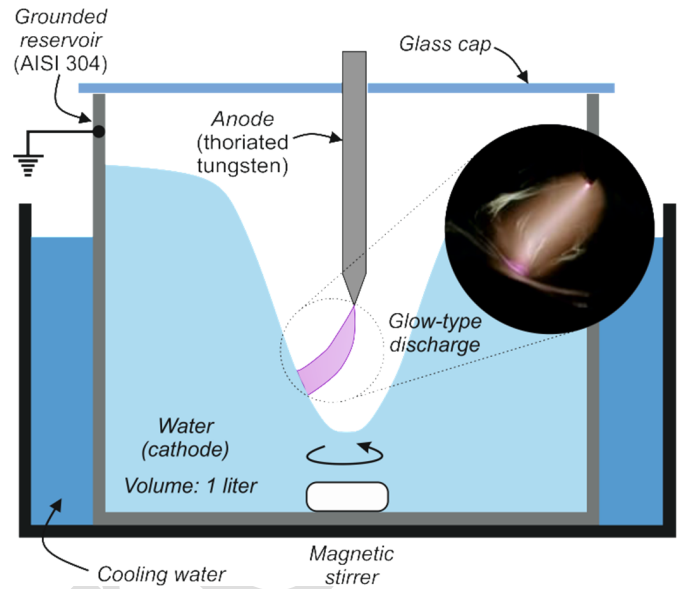


Fig. 1. Experimental arrangement. A photograph of the discharge is shown in the inset.

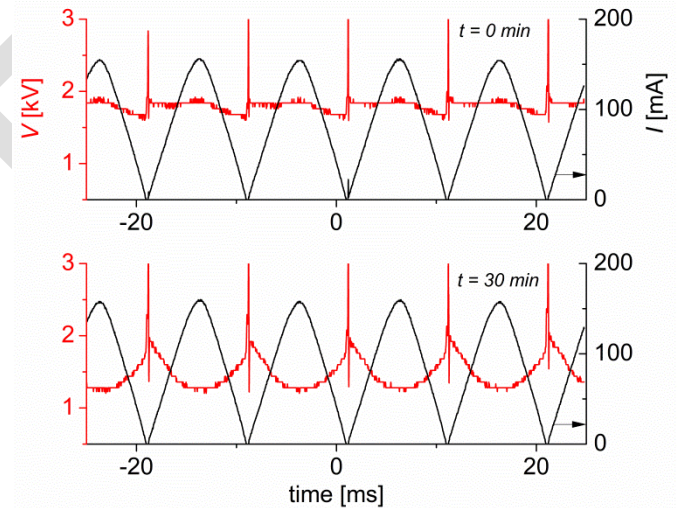


Fig. 2. Voltage (V) and current (I) oscillograms for $t = 0$ min and $t = 30$ min.

122 was kept constant at about 20°C by means of a cooling
 123 system, due to the thermally fragile chemistry of H_2O_2 [14].
 124 No significant changes in PAW volume were observed after the
 125 synthesis (<5 mL).

126 The power supply was a high-voltage transformer (25 kV,
 127 50 Hz) with a high dispersion reactance (65 ± 2 k Ω).
 128 The output of the transformer was connected to the reactor
 129 through a semiconductor full-wave rectifier to define the
 130 polarity of the electrodes. The voltage and current signals
 131 were recorded through a four-channel oscilloscope (Tektronix
 132 TDS 2004C, sampling rate 1 GS s^{-1} , bandwidth 70 MHz)
 133 by using a resistive–capacitive voltage divider (Tektronix
 134 P6015A, 1000X, 3 pF, 100 M Ω) and a low-inductance shunt
 135 resistance (100 Ω), respectively.

136 Fig. 2 shows the voltage (V) and current (I) oscillograms at
 137 the beginning ($t = 0$ min) and after 30 min of water activation

($t = 30$ min). The discharge is likely ignited by a streamer-to-spark high-voltage transition (voltage spikes up to ~ 8 kV are found at the beginning of each pulse) [5]. A transient positive corona discharge (cathode-directed streamer development) is formed near the metal pin electrode before sparking, but soon after the breakdown, the voltage drops to several hundred volts due to the high impedance of the transformer, and the discharge stabilizes. The discharge was operated in a millisecond pulsed-dc regime at a constant rms value of 100 mA.

The measured voltage in Fig. 2 includes not only the drop in the gas gap but also the drop in the equivalent resistance of the water electrode. At 0 min, the V - I characteristic curve has a positive slope, reaching a maximum voltage value of about 2 kV, while at 30 min, the slope becomes negative and the voltage drops to about 1.2 kV. This is expected because as the exposure time increases, the conductivity of the water increases (due to the formation of ions in the liquid), and therefore, the resistive voltage drop in the water becomes small compared to that of the gas. The discharge operating power was then calculated from the voltage and current signals at $t = 30$ min. The resulting power was ≈ 100 W.

The found voltage (of about 1.2 kV) for the ≈ 10 mm gas gap is consistent with the cathode voltage drop measurements (600–900 V) reported in the literature for similar discharges [15]. (An axial electric field of 20–40 V/mm can be expected in the positive column under the conditions considered [16]). As a whole, the V - I characteristic curve together with the emissive structure of the discharge (inset of Fig. 1) suggests that the studied discharge has many properties in common with the atmospheric pressure glow-type discharge between two metal electrodes [17] (e.g., the review [5] and references therein). This type of water-cathode discharge is most often referred to as a glow (-like) discharge, but also sometimes as an arc discharge [15]. Moreover, the negative V - I characteristic after 30 min of water activation ($t = 30$ min) (Fig. 2) suggests that for high currents, the predominant ionization mechanism corresponds to associative ionization involving nitrogen and oxygen atoms, which is independent of the reduced electric field. In this sense, the high-temperature values reported by other authors in the gas (≈ 2000 – 4000 K) [15] are in agreement with the hypothesis that charge reproduction occurs mainly by associative ionization in atomic collisions (rather than by electron-impact ionization), thus explaining the negative V - I characteristic [16], [18].

No noticeable damage was observed on the metal electrode after several experiments (the electrode erosion is negligible under the experimental conditions considered, and no electrode material—metal vapor—is introduced into the discharge).

III. TREATMENTS AND PHYSICOCHEMICAL DETERMINATIONS

Two treatments were used during the experiments.

- 1) Covering the container with a glass cap during the activation process (closed reactor). Confined air volume ≈ 330 mL.

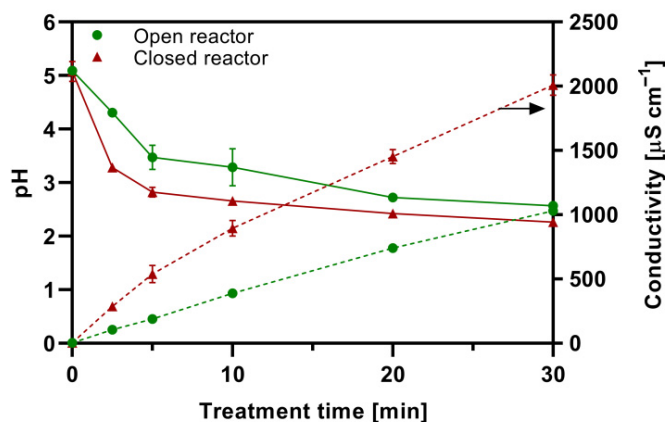


Fig. 3. pH and electrical conductivity of PAW as a function of treatment time (min).

- 2) Without covering the container (open reactor).

The substantial difference between the two treatments resides in the availability of fresh air: when the glass cap is placed on the container, a closed gas chamber is formed where the discharge is established, and the air molecules are consumed, resulting in the formation of different RONS.

A pH meter (Hanna HI 8314) and a conductivity meter (Oakton Cyberscan Cond 610), previously calibrated, were used to measure the pH and electrical conductivity, respectively, while the protocols established in the standard methods for the examination of water and wastewater [19] were followed to measure the concentrations of NO_3^- , NO_2^- , and H_2O_2 in the aqueous phase. Briefly, H_2O_2 concentration was measured using a peroxidase, which catalyzed the reaction of H_2O_2 with 4-aminophenazone and phenol giving a red product (measured at 505 nm). The UV method (absorbances at 220 and 275 nm) was used for NO_3^- measurements and NO_2^- concentrations were quantified following the Griess technique. Measurements were done with a spectrophotometer UV-VIS Spectrum SP-2100.

Measurements were done in triplicate for each time studied (2.5, 5, 10, 20, and 30 min). PAW stability in the postdischarge phase was followed for 90 days. PAW samples were stored at 4 °C in amber flasks, tightly capped, and in the dark. Data are shown as mean value \pm standard error of the mean (SEM). The distilled water from which the PAW was generated had a $\text{pH} \approx 5$ and a conductivity ≤ 5 $\mu\text{S}/\text{cm}$.

IV. RESULTS

Fig. 3 shows that pH decreases and electrical conductivity increases with plasma exposure time (treatment time).

The pH reached values of 2.3 and 2.6 at 30 min, for closed and open reactors, respectively, while the electrical conductivity increased approximately linearly with time for both treatments, although with a large difference between their values after the treatment. For the closed reactor, a conductivity value of ≈ 2000 $\mu\text{S}/\text{cm}$ was reached, while for the open reactor, it was ≈ 1000 $\mu\text{S}/\text{cm}$. The decrease in pH and the increase in conductivity are related to the formation of acids (HNO_2 and HNO_3) and ions (mainly H^+ and

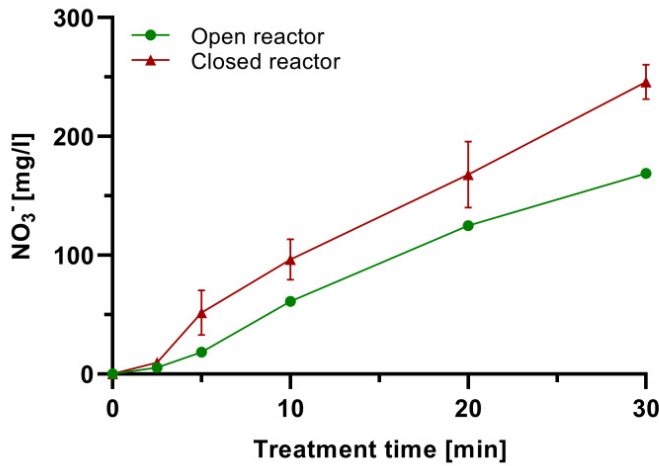


Fig. 4. NO_3^- concentration as a function of treatment time (min).

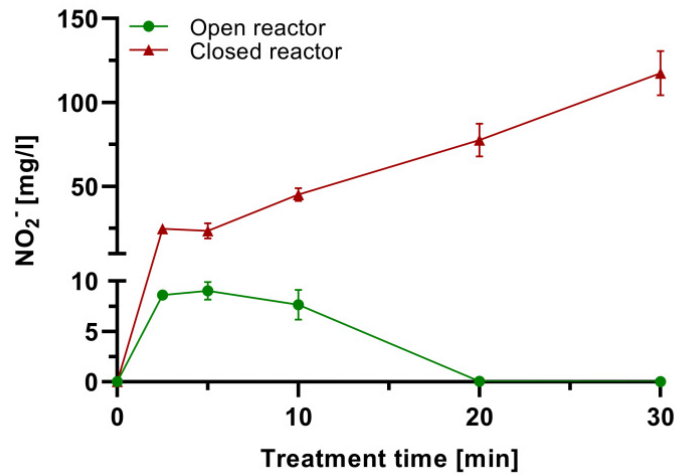


Fig. 5. NO_2^- concentration as a function of treatment time (min).

233 NO_3^-) in the liquid volume and are characteristic in water
 234 in contact with nonthermal discharges in air and similar
 235 mixtures [20].

236 Fig. 4 shows the concentration of NO_3^- in the aqueous
 237 phase, and it is evident that for both treatments, it grows
 238 approximately linearly with time. The maximum values
 239 reached at 30 min were ≈ 250 mg/L for the closed reactor and
 240 ≈ 170 mg/L for the open reactor. These high values of NO_3^-
 241 show the potential of activated water for use as fertilizer [21].

242 DC-excited discharges in a pin-to-water electrode geometry
 243 operating in air at rms current values of 100 mA and a
 244 power of 100 W (see the inset of Fig. 1) typically exhibit
 245 gas temperatures exceeding 3000 K, electron temperatures of
 246 ≈ 1 eV, and small ionization degrees ($\sim 10^{-5}$) [6]. Under such
 247 high gas temperatures and low ionization plasma conditions,
 248 the atomic species N and O are produced mainly in the hottest
 249 parts of the discharge by collisions among heavy species ($\text{O}_2 +$
 250 $\text{M} \rightarrow \text{O} + \text{O} + \text{M}$; $\text{N}_2 + \text{M} \rightarrow \text{N} + \text{N} + \text{M}$, being
 251 M a third body), rather than by electron-impact dissociation
 252 (e.g., [17], [18]). These, in turn, combine to form NO (via the
 253 Zeldovich mechanism [1]) and NO_2 , which could then enter
 254 from the gas phase to the liquid by diffusion and react with
 255 water molecules to form NO_3^- (and also NO_2^-) in the liquid.
 256 However, even with much lower concentration in gas phase
 257 than NO and NO_2 , the gaseous HNO_2 may also play a relevant
 258 role in the formation of NO_2^- in the aqueous phase since its
 259 Henry's coefficient is four and five orders of magnitude larger
 260 than that of NO_2 and NO, respectively [22].

261 Fig. 5 shows that the concentration of NO_2^- presents very
 262 different behaviors between treatments: while in the closed
 263 reactor, it grows monotonically, in the open reactor, it grows
 264 during the first 2.5 min to a maximum value and then decreases
 265 until it is extinguished. For the closed reactor, the maximum
 266 value was 120 mg/L at 30 min of treatment, while in the
 267 open reactor treatment, it reaches a peak value of ≈ 7 mg/L at
 268 2.5 min and disappears at 20 min.

269 Fig. 6 shows the concentration of H_2O_2 as a function of
 270 treatment time. A behavior similar to that of nitrite, but inverse

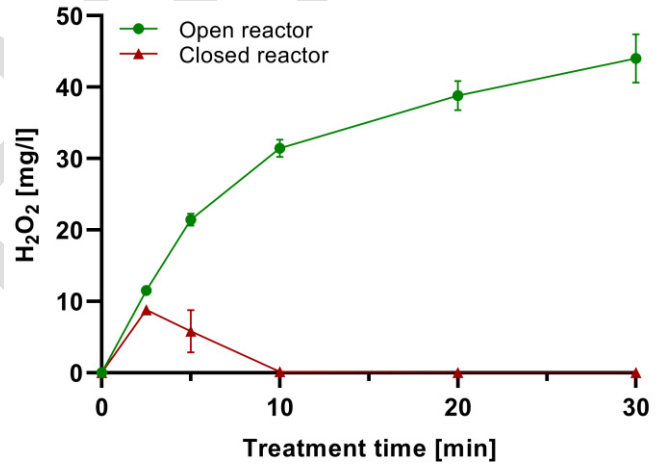
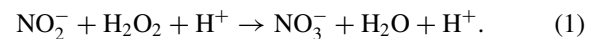


Fig. 6. H_2O_2 concentration as a function of activation time (min).

with respect to the treatments, is observed. For the open
 271 reactor, the concentration increases monotonically, reaching
 272 ≈ 40 mg/L at 30 min, while in the closed reactor, a maximum
 273 ≈ 10 mg/L is reached at 2.5 min and then decays to extinction
 274 for times greater than 10 min.
 275

276 The chemistry in the aqueous phase is strongly related
 277 to the transient RONS chemistry in the gas phase, which
 278 in turn depends on the operating conditions of the reactor.
 279 The NO_2^- and H_2O_2 species react with each other to form
 280 peroxyntitrous acid (ONOOH), the rate of this reaction being
 281 strongly dependent on the pH, occurring at much higher rates
 282 the lower the pH [23], [24]



283
 284 The elevated aqueous concentrations of hydrogen peroxide
 285 observed in open air reactor conditions suggest that in this
 286 configuration, some long-lived RONS (i.e., gas-phase reaction
 287 timescales \ll diffusion timescales), such as NO_2 and HNO_2 ,
 288 which in turn are responsible for the creation of nitrite (and
 289 also nitrate) in the liquid phase, do not accumulate in the gas
 290 phase due to the diffusion of species into the surrounding

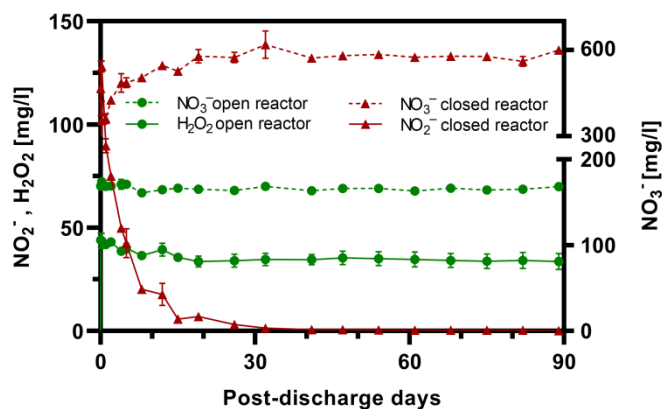
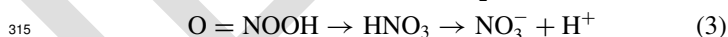


Fig. 7. Concentration of the reactive species in the postdischarge phase for the closed and open reactors.

291 ambient air. The diffusion timescale ($\equiv d^2/D$, being $d \sim$
 292 1 cm the thickness of the afterglow region and $D \sim 10^{-5}$ m²/s
 293 the diffusion coefficient of species in air at 300 K [1]) is
 294 of the order of 1 s under the conditions considered. There-
 295 fore, the concentration of NO₂⁻ in PAW remains low enough
 296 (while the pH is not very low) to almost suppress the decom-
 297 position of H₂O₂ by nitrites under acidic conditions, according
 298 to pathway (1). On the other hand, the higher levels of NO₃⁻
 299 observed for the closed reactor conditions (Fig. 4) suggest that
 300 the air confinement allows the accumulation of such long-lived
 301 RONS in the gas phase, which in turn produce a rapid growth
 302 in the concentration of NO₂⁻ (and also a reduction in the pH)
 303 with the consequent fast degradation of H₂O₂. It should be
 304 noted that the highly reactive hydroxyl radical has gas-phase
 305 reaction rates with timescales much shorter than diffusion (i.e.,
 306 their losses are dominated by gas-phase kinetics rather than
 307 diffusion); thus, it is not expected to accumulate, regardless of
 308 the mode of operation of the reactor. Note that the combination
 309 of dissolved OH⁻ radicals is likely the main formation pathway
 310 of aqueous H₂O₂ in a plasma-liquid system with liquid as
 311 cathode [25].

312 The ONOOH molecule is unstable and degrades faster the
 313 lower the pH. It has two paths of destruction



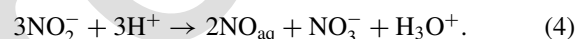
316 and one of them gives as a by-product an OH⁻ radical.
 317 This species is of particular importance in disinfection and
 318 decontamination processes because it is highly reactive [7].

319 In this sense, the mixture of PAW generated in the reac-
 320 tor under open and closed operating conditions becomes
 321 an alternative with great potential in disinfection processes,
 322 degradation of contaminants, and elimination of bacteria or
 323 pathogens due to the availability of OH⁻ radicals in solution
 324 via reaction (2).

325 Fig. 7 shows the concentrations of the reactive species in
 326 the postdischarge phase for both treatments.

327 For the open reactor, hydrogen peroxide decays slightly in
 328 the first 20 days and then remains stable until 90 days, while

329 nitrate remained constant all the period (it is worth mentioning
 330 that for this treatment, there is no nitrite immediately after
 331 30 min of exposure). In the closed reactor, where there
 332 is no hydrogen peroxide in the postdischarge phase, nitrate
 333 increases up to ≈ 600 mg/L during the first 30 days and then
 334 remains stable for 90 days, while nitrite drops rapidly until it
 335 disappears after one month. Disappearance in nitrite is to be
 336 expected since it is unstable in acidic pH, mostly due to its
 337 transformation to nitrate [20]. Tachibana and Nakamura [10]
 338 generated four types of PAW: from deionized water and from
 339 drinking water, with high and low NO_X⁻ concentrations ($X = 2,$
 340 3). The authors report that, for low pH, nitrite disappears after
 341 several days (between 6 and 40), while for pH close to 7, the
 342 concentrations of both species remain stable after 40 days and
 343 attribute that nitrite is completely converted to nitrate through
 344 several ionic reactions, the following being predominant for
 345 storage times of the order of several days:



347 V. CONCLUSION

348 Physicochemical properties were measured in PAW with a
 349 nonthermal glow-type discharge in atmospheric pressure air
 350 with a water cathode. The determinations were performed dur-
 351 ing the activation process and postdischarge (up to 90 days).
 352 Two variants (treatments) were used: 1) with the gaseous
 353 chamber where the glow discharge is set confined (closed
 354 reactor) and 2) with the open chamber (open reactor). The
 355 volume treated was 1 L and the maximum exposure time was
 356 30 min. The results are given as follows.

- 357 1) The concentration of NO₃⁻ in the aqueous phase
 358 increased with the activation time, reaching maximum
 359 concentrations of ≈ 250 mg/L for the closed reactor and
 360 ≈ 170 mg/L for open reactor.
- 361 2) The concentration of NO₂⁻ in the closed reactor
 362 increased with treatment time (≈ 120 mg/L at 30 min),
 363 while in the open reactor, NO₂⁻ presented a maximum at
 364 ≈ 5 min and then decreased until its extinction at 20 min.
- 365 3) H₂O₂ concentration in the open reactor increased with
 366 activation time (≈ 45 mg/L at 30 min), while in the
 367 closed reactor, it showed a maximum at 2 and
 368 5 min (≈ 9 mg/L) and then disappeared for longer
 369 times.
- 370 4) pH decreased and electrical conductivity increased with
 371 activation time for both reactors. The minimum pH val-
 372 ues were ≈ 2 and 2 for closed reactor and ≈ 2 and 5 for
 373 open reactor; while the maximum conductivity values
 374 were 2010 $\mu\text{S}/\text{cm}$ (closed reactor) and 1030 $\mu\text{S}/\text{cm}$
 375 (open reactor).
- 376 5) In the postdischarge phase, the concentrations of NO₃⁻
 377 and H₂O₂ remained practically constant for up to
 378 90 days for the open reactor, while in the closed
 379 reactor, NO₂⁻ concentration decreased markedly until
 380 it disappeared at approximately 30 days, while NO₃⁻
 381 concentration increased simultaneously.

ACKNOWLEDGMENT

Author Contributions: conceptualization: Brenda Santamaría, Matías G. Ferreyra, and Leandro Prevosto; methodology: Brenda Santamaría, Matías G. Ferreyra, Juan C. Chamorro, Ezequiel Cejas, and Brenda L. Fina; software: Brenda Santamaría, Matías G. Ferreyra, and Brenda L. Fina; writing—original draft preparation: Brenda Santamaría and Matías G. Ferreyra; writing—review: Juan C. Chamorro, Ezequiel Cejas, Brenda L. Fina, and Leandro Prevosto; and funding acquisition: Brenda L. Fina and Leandro Prevosto.

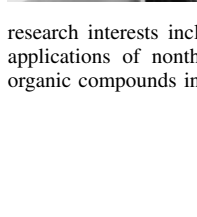
Brenda L. Fina and Leandro Prevosto are members of the Consejo Nacional de Investigaciones Científicas y Técnicas (CONICET).

REFERENCES

- [1] Y. P. Raizer, *Gas Discharge Physics*, 1st ed. Berlin, Germany: Springer, 1991.
- [2] M. I. Boulos, P. Fauchais, and E. Pfender, *Thermal Plasmas: Fundamentals and Applications*, vol. 1, 1st ed. 1994.
- [3] A. Fridman, A. Chirokov, and A. Gutsol, "Non-thermal atmospheric pressure discharges," *J. Phys. D: Appl. Phys.*, vol. 38, no. 2, pp. 1–24, Jan. 2005, doi: [10.1088/0022-3727/38/2/R01](https://doi.org/10.1088/0022-3727/38/2/R01).
- [4] I. Adamovich et al., "The 2017 plasma roadmap: Low temperature plasma science and technology," *J. Phys. D: Appl. Phys.*, vol. 50, no. 32, Aug. 2017, Art. no. 323001, doi: [10.1088/1361-6463/aa76f5](https://doi.org/10.1088/1361-6463/aa76f5).
- [5] P. Bruggeman and C. Leys, "Non-thermal plasmas in and in contact with liquids," *J. Phys. D: Appl. Phys.*, vol. 42, no. 5, Mar. 2009, Art. no. 053001, doi: [10.1088/0022-3727/42/5/053001](https://doi.org/10.1088/0022-3727/42/5/053001).
- [6] P. J. Bruggeman et al., "Plasma–liquid interactions: A review and roadmap," *Plasma Sources Sci. Technol.*, vol. 25, no. 5, Sep. 2016, Art. no. 053002, doi: [10.1088/0963-0252/25/5/053002](https://doi.org/10.1088/0963-0252/25/5/053002).
- [7] M. G. Ferreyra et al., "Indigo carmine degradation in water induced by a pulsed positive corona discharge in air: Discharge and post-discharge effects," *Plasma*, vol. 5, no. 2, pp. 265–279, May 2022, doi: [10.3390/plasma5020021](https://doi.org/10.3390/plasma5020021).
- [8] A. P. S. Crema, L. D. P. Borges, G. A. Micke, and N. A. Debacher, "Degradation of Indigo carmine in water induced by non-thermal plasma, ozone and hydrogen peroxide: A comparative study and by-product identification," *Chemosphere*, vol. 244, Apr. 2020, Art. no. 125502, doi: [10.1016/j.chemosphere.2019.125502](https://doi.org/10.1016/j.chemosphere.2019.125502).
- [9] D. Guo, H. Liu, L. Zhou, J. Xie, and C. He, "Plasma-activated water production and its application in agriculture," *J. Sci. Food Agric.*, vol. 101, no. 12, pp. 4891–4899, Sep. 2021, doi: [10.1002/jsfa.11258](https://doi.org/10.1002/jsfa.11258).
- [10] K. Tachibana and T. Nakamura, "Comparative study of discharge schemes for production rates and ratios of reactive oxygen and nitrogen species in plasma activated water," *J. Phys. D: Appl. Phys.*, vol. 52, no. 38, Sep. 2019, Art. no. 385202, doi: [10.1088/1361-6463/ab2529](https://doi.org/10.1088/1361-6463/ab2529).
- [11] P. Bruggeman, J. Liu, J. Degroote, M. G. Kong, J. Vierendeels, and C. Leys, "DC excited glow discharges in atmospheric pressure air in pin-to-water electrode systems," *J. Phys. D: Appl. Phys.*, vol. 41, no. 21, Nov. 2008, Art. no. 215201, doi: [10.1088/0022-3727/41/21/215201](https://doi.org/10.1088/0022-3727/41/21/215201).
- [12] A. J. M. Pemen et al., "Power modulator for high-yield production of plasma-activated water," *IEEE Trans. Plasma Sci.*, vol. 45, no. 10, pp. 2725–2733, Oct. 2017, doi: [10.1109/TPS.2017.2739484](https://doi.org/10.1109/TPS.2017.2739484).
- [13] X. Li et al., "Comparison of deionized and tap water activated with an atmospheric pressure glow discharge," *Phys. Plasmas*, vol. 26, no. 3, Mar. 2019, Art. no. 033507, doi: [10.1063/1.5080184](https://doi.org/10.1063/1.5080184).
- [14] W. F. L. M. Hoeben, P. P. van Ooij, D. C. Schram, T. Huiskamp, A. J. M. Pemen, and P. Lukes, "On the possibilities of straightforward characterization of plasma activated water," *Plasma Chem. Plasma Process.*, vol. 39, no. 3, pp. 597–626, May 2019, doi: [10.1007/s11090-019-09976-7](https://doi.org/10.1007/s11090-019-09976-7).
- [15] P. Bruggeman et al., "Characteristics of atmospheric pressure air discharges with a liquid cathode and a metal anode," *Plasma Sources Sci. Technol.*, vol. 17, no. 2, May 2008, Art. no. 025012, doi: [10.1088/0963-0252/17/2/025012](https://doi.org/10.1088/0963-0252/17/2/025012).
- [16] L. Prevosto, H. Kelly, B. Mancinelli, J. C. Chamorro, and E. Cejas, "On the physical processes ruling an atmospheric pressure air glow discharge operating in an intermediate current regime," *Phys. Plasmas*, vol. 22, no. 2, Feb. 2015, Art. no. 023504, doi: [10.1063/1.4907661](https://doi.org/10.1063/1.4907661).
- [17] E. Cejas, J. C. Chamorro, and L. Prevosto, "Quantitative Schlieren diagnostics applied to a millisecond pulsed-DC hybrid discharge in atmospheric pressure air," *Plasma Chem. Plasma Process.*, vol. 42, no. 3, pp. 657–670, May 2022, doi: [10.1007/s11090-022-10233-7](https://doi.org/10.1007/s11090-022-10233-7).
- [18] M. S. Benilov and G. V. Naidis, "Modelling of low-current discharges in atmospheric-pressure air taking account of non-equilibrium effects," *J. Phys. D: Appl. Phys.*, vol. 36, no. 15, pp. 1834–1841, Aug. 2003, doi: [10.1088/0022-3727/36/15/314](https://doi.org/10.1088/0022-3727/36/15/314).
- [19] R. B. Baird, A. D. Eaton, and E. W. Rice, *Standard Methods for the Examination of Water and Wastewater*, 23rd ed. Washington DC, USA: American Public Health Association, 2017.
- [20] P. Lukes, B. R. Locke, and J. L. Brisset, "Aqueous-phase chemistry of electrical discharge plasma in water and in gas-liquid environments," *Plasma Chem. Catal. Gases Liquids*, vol. 1, pp. 243–308, Aug. 2012, doi: [10.1002/9783527649525.ch7](https://doi.org/10.1002/9783527649525.ch7).
- [21] P. Ranieri et al., "Plasma agriculture: Review from the perspective of the plant and its ecosystem," *Plasma Processes Polym.*, vol. 18, no. 1, Jan. 2021, Art. no. 2000162, doi: [10.1002/ppap.202000162](https://doi.org/10.1002/ppap.202000162).
- [22] M. Janda, K. Hensel, P. Tóth, M. E. Hassan, and Z. Machala, "The role of HNO₂ in the generation of plasma-activated water by air transient spark discharge," *Appl. Sci.*, vol. 11, no. 15, p. 7053, Jul. 2021, doi: [10.3390/app11157053](https://doi.org/10.3390/app11157053).
- [23] P. Lukes, E. Dolezalova, I. Sisrova, and M. Clupek, "Aqueous-phase chemistry and bactericidal effects from an air discharge plasma in contact with water: Evidence for the formation of peroxyxynitrite through a pseudo-second-order post-discharge reaction of H₂O₂ and HNO₂," *Plasma Sources Sci. Technol.*, vol. 23, no. 1, Feb. 2014, Art. no. 015019, doi: [10.1088/0963-0252/23/1/015019](https://doi.org/10.1088/0963-0252/23/1/015019).
- [24] D. E. Damschen and L. R. Martin, "Aqueous aerosol oxidation of nitrous acid by O₂, O₃ and H₂O₂," *Atmos. Environ.*, vol. 17, no. 10, pp. 2005–2011, 1983, doi: [10.1016/0004-6981\(83\)90357-8](https://doi.org/10.1016/0004-6981(83)90357-8).
- [25] X. He et al., "The formation pathways of aqueous hydrogen peroxide in a plasma-liquid system with liquid as the cathode," *Plasma Sources Sci. Technol.*, vol. 27, no. 8, Aug. 2018, Art. no. 085010, doi: [10.1088/1361-6595/aad66d](https://doi.org/10.1088/1361-6595/aad66d).



Brenda Santamaría was born in Venado Tuerto, Argentina, in 1989. She received the Engineering degree in chemical engineering from the Rosario Regional Faculty, National Technological University, Rosario, Argentina, in 2020.



Since 2021, she has been a Doctoral Fellow with the Consejo Nacional de Investigaciones Científicas y Técnicas (CONICET), Venado Tuerto. She is currently conducting doctoral studies with the Electrical Discharge Group (GDE), National Technological University, Venado Tuerto. Her current

research interests include nonthermal discharge in contact with liquids and applications of nonthermal plasma, in particular, and decontamination of organic compounds in water.

Matías G. Ferreyra was born in Canals, Argentina, in 1992. He received the Engineering degree in electromechanical engineering from the Venado Tuerto Regional Faculty, National Technological University, Venado Tuerto, Argentina, in 2018.

Since 2019, he has been a Doctoral Fellow with the Consejo Nacional de Investigaciones Científicas y Técnicas (CONICET), Venado Tuerto. He is currently conducting doctoral studies with the Electrical Discharge Group (GDE), National Technological University, and the Institute of Agricultural and Environmental Biosciences Research (INBA), Faculty of Agronomy, University of Buenos Aires, Ciudad Autónoma de Buenos Aires, Argentina. Since 2022, he has been a Professor with the National Technological University. His current research interests include nonthermal discharge in contact with liquids, agriculture applications of plasma activated water, optical diagnostics, and plasma technology.

518
519
520
521
522
523
524
525
526
527
528
529
530
531
532

Juan C. Chamorro was born in Riosucio, Colombia, in March 1989. He received the bachelor's degree in physics engineering from the Technological University of Pereira, Pereira, Colombia, in 2013, and the Ph.D. degree in engineering from the National University of Rosario, Rosario, Argentina, in 2021.

Since 2014, he has been a part of the Electrical Discharge Group, and since 2019, he has been a Professor with the National Technological University, Venado Tuerto, Argentina. Currently, he holds a Postdoctoral Fellowship from the Consejo Nacional de Investigaciones Científicas y Técnicas (CONICET), Venado Tuerto. His current research focuses on plasma optical diagnostics, computational modeling, and the applications of nonthermal discharges.

533
534
535
536
537
538
539
540
541
542
543
544
545
546
547
548

Ezequiel Cejas was born in Los Quirquinchos, Argentina, in 1987. He received the Engineering degree in electromechanical engineering from the Venado Tuerto Regional Faculty, National Technological University, Venado Tuerto, Argentina, in 2017, and the Ph.D. degree in engineering from the National University of Rosario, Rosario, Argentina, in 2022.

Since 2022, he has been a Post-Doctoral Fellow with the Consejo Nacional de Investigaciones Científicas y Técnicas (CONICET), Venado Tuerto. He is conducting post-doctoral studies in the area of food preservation and alimentary security employed nonthermal plasmas at atmospheric pressure with the Electrical Discharge Group, National Technological University. His current research interests include plasma diagnostics, numerical modeling, and plasma technology.



Brenda L. Fina was born in Colón, Argentina, in 1986. She received the Diploma degree in biotechnology and the Ph.D. degree in biological sciences from Rosario National University, Rosario, Argentina, in 2010 and 2015, respectively.

She has been a Professor at Rosario National University. Currently, she is at the National Technological University, where she is a part of the Electrical Discharge Group. Since 2021, she has been a Researcher at the Consejo Nacional de Investigaciones Científicas y Técnicas (CONICET), Venado Tuerto, Argentina. She has worked on toxicological studies of fluoride in plants and animals, and her current research interests include the biological applications of nonthermal plasma, including microbial disinfection, decontamination of organic compounds in water, and the application of activated water in seeds and fruits.

549
550
551
552
553
554
555
556
557
558
559
560
561
562
563
564

Leandro Prevosto was born in Venado Tuerto, Argentina, in 1971. He received the Diploma degree in electromechanical engineering from the National Technological University, Venado Tuerto, in 2005, and the Ph.D. degree (Hons.) in engineering from the University of Buenos Aires, Buenos Aires, Argentina, in 2009.

Since 2010, he has been a Professor with the National Technological University, where he is currently the Director of the Electrical Discharge Group. Since 2012, he has been a Researcher with the Consejo Nacional de Ciencias y Tecnología (CONICET), Venado Tuerto. His current research interests include thermal and nonthermal electrical discharges, plasma diagnostics, and plasma applications, including plasmas in agriculture.

565
566
567
568
569
570
571
572
573
574
575
576
577
578
579